A ***tris***(8-hydroxyquinoline) aluminum-based organic bistable device using ITO surfaces modified by Ag nanoparticles

2013 J. Phys. D: Appl. Phys. 46 445107

(http://iopscience.iop.org/0022-3727/46/44/445107)

IOP PUBLISHING JOURNAL OF PHYSICS D: APPLIED PHYSICS

J. Phys. D: Appl. Phys. **46** (2013) 445107 (6pp) doi:10.1088/0022-3727/46/44/445107

A *tris*(8-hydroxyquinoline) aluminum-based organic bistable device using ITO surfaces modified by Ag nanoparticles

Bo Jiao, Zhaoxin Wu[1], Hua Dong, Shuya Ning and Xun Hou

Shaanxi Key Laboratory of Photonics Technology for Information, Key Laboratory for Physical Electronics and Devices of the Ministry of Education, School of Electronic and Information Engineering, Xi'an Jiaotong University, Xi'an, Shaanxi, 710049, People's Republic of China

E-mail: zhaoxinwu@mail.xjtu.edu.cn

Received 17 May 2013, in final form 29 August 2013
Published 17 October 2013
Online at stacks.iop.org/JPhysD/46/445107

Abstract

A *tris*(8-hydroxyquinoline) aluminum (Alq_3)-based organic bistable device (OBD) using Al electrode and ITO electrode modified by Ag nanoparticles (NPs) was reported. The OBD exhibits high ON/OFF switching ratios in the range of 10^2–10^3 and long retention time over 10^4 s. The influence of the Ag NPs densities, as well as the Alq_3 film thickness on the switch performance current–voltage (I–V) of the OBDs was studied. Correlation between filament formation mechanism and charge storage mechanism was observed by analysing the I–V characteristics of OBDs with different Alq_3 film thickness. As for the Alq_3 film with thickness of 300 nm, the trapping effect of Ag NPs leads to both ON and OFF states for OBD; for 100 nm thick Alq_3 film, the effect of filamentation dominates in the ON and OFF states of OBD. For the case of 200 nm thick Alq_3 film, however, the ON state results from the filamentation effect, while trapping effect is responsible for the OFF state. In addition, the diffusion effect of Al atoms in Alq_3 film in the devices was discussed and was expected to explain this thickness-dependence relationship.

(Some figures may appear in colour only in the online journal)

1. Introduction

Recently, there has been growing interest in organic bistable devices (OBDs) due to their advantage of simple device structure, low fabrication cost and large variation of organic chemical structure [1–3]. Electrical bistable phenomena have been demonstrated in various devices with different architectures [4–20], such as metal nanoparticles (NPs)-based OBDs [4, 13, 21–24] metal–insulator–metal (MIM) OBDs [25–28], organic-based donor–acceptor OBDs [8], supramolecular structure OBDs [5], and organic ferroelectric OBD [18, 19, 29–31] *et al*. In OBDs based on metal NPs, Au-NPs [20, 22], Ag-NPs [13], and Al-NPs [32], all have been selected to generate electrically switching behaviour. For those devices, it has been demonstrated that the NP or cluster morphology of the metal material is crucial for switch performance [20, 32]. However, the influence of organic active layer thickness, as well as the density of metal NPs on the performance of OBDs have received scarce attention. The understanding of the relevant switching mechanisms in metal NPs-based OBDs is still a topic of active debate. Typically, there are two totally different mechanisms for the electrical bistable phenomena of OBDs. One is filament formation mechanism [10, 26–27], in which many low-resistance pathways formed by metallic filaments. The different conduction states switched as the number of the metallic filaments changes. In the filament formation mechanism, the current (I) of the OBD should exhibit a linear-dependence on the applied voltage (V) in the bistable region. Another is charge storage mechanism

[1] Author to whom any correspondence should be addressed.

[23, 33–35], in which the bistable phenomenon was ascribed to charge trapping sites in OBD, and conduction state switched as these trapping sites were charged or discharged. In the charge storage mechanism, the I–V characteristic in the bistable region should exhibit a quadratic or nearly quadratic relationship. The correlation between filament formation mechanism and charge storage mechanism, however, is seldom reported. For OBDs based on metal NPs, such as Au NPs-based OBD [22], Al NPs-based OBD [21, 23], and Ag NPs-based OBD [13], it was always believed that metal NPs act as charge trapping sites in the OBD [23], and the role of metal NPs is independent of the thickness of the organic active layer [13, 25].

In this paper, we reported on an OBD using Al electrode and ITO electrode modified by Ag NPs. *Tris*(8-hydroxyquinoline) aluminum (Alq_3), a typical organic electron-transporting material in organic light-emitting diodes, was used as the organic active layer. By analysing the I–V characteristics of OBDs with different Alq_3 film thickness, as well as with different Ag NPs densities, the correlation between filament formation mechanism and charge storage mechanism was observed. Tests by applying cyclic sequential WRITE–READ–ERASE–READ voltage pulses with different write (erase) time section were used to deduce the write (erase) time of OBDs with different thickness of Alq_3 film. Data retention measurements under stress conditions for OBDs with different thickness of Alq_3 film were also carried out to examine the potential in the data-storage application of those devices.

2. Experiments and discussion

As shown in figure 1(*a*), OBDs proposed in this study consist of a single Alq_3 layer interposed between Al electrode and ITO electrode modified by Ag NPs. Al was used as the anode and ITO as the cathode. The Ag NPs-attached on an ITO substrate were prepared by a solution-based surface assemble process referred to in the work of Lukomska *et al* [36]. A solution of silver nitrate (45 mg in 200 ml H_2O) was stirred at 60 °C, and then trisodium citrate (6 ml, 34 mm) was added dropwise to the solution. Heating the reaction mixture to 85 °C, and 675 mg polyvinylpyrrolidone (PVP) was added as dispersant, then the solution was stirred for 1 h until the colour of reaction mixture turned to a yellowish brown. The colloidal solution was centrifuged at 2500 rpm for 30 min, which produced a precipitate containing uniform NPs with the diameter of 50 nm. In order to obtain the different density of NPs, three groups glass-coated 100 nm thick ITO were dipped into a 2% aqueous solution of 3-aminopropyltriethoxy-silane (APS) for 5 h (substrate S1), 2 h (substrate S2) and 1 h (substrate S3) at room temperature, respectively. Then the three groups APS-coated ITO glass were kept immersed in the silver colloidal solution at room temperature. The group of substrate S1 was kept immersed for 48 h, and substrate S2 was kept immersed for 24 h, and substrate S3 was kept immersed for 12 h. All substrates were annealed in a vacuum drying oven at temperatures of 160 °C for 5 h. Figure 1(*b*) shows the atomic force microscopy (AFM) image of surface of ITO modified by Ag NPs. As shown in

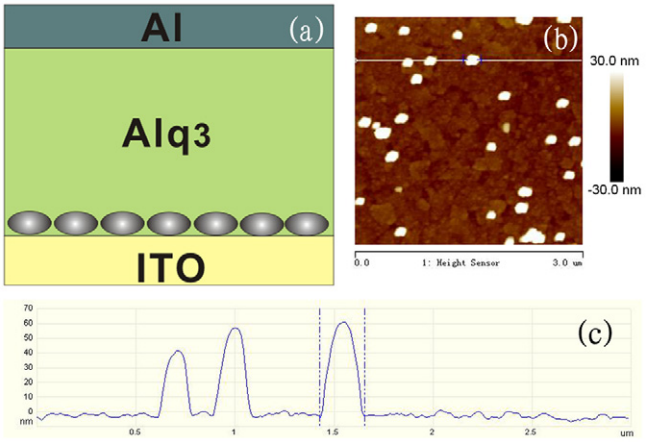

Figure 1. The schematic diagrams of cross section view of the OBD in this study (*a*). The tapping-mode AFM images of the surface of ITO modified by Ag NPs (*b*). Height image of the Ag NPs along the line section in (*b*) is also shown (*c*). (Scan size: $3 \times 3\ \mu$m).

the height image of figure 1(*c*), the diameters of the Ag NPs vary from 40 to 60 nm. Alq_3 film and Al electrode were grown sequentially by thermal evaporation without vacuum break. The pressure during thermal evaporation for deposition was about 5×10^{-4} Pa. All fabrication processes were carried out in the 100-level clean room. Thus, the influence of dust on the switch performance of OBDs can be neglected [37]. The thickness of the films was determined *in situ* by a quartz-crystal sensor and *ex situ* by a profilometer. Active area of devices was 12 mm^2 for all the samples studied in this work. The current–voltage (I–V) curves and the retention time under stress condition characteristics of the devices were measured by a computer-controlled sourcemeter (Keithley 2602). All the measurements were carried out at room temperature under ambient conditions.

In our study, three types ITO modified with different densities Ag NPs (S1, S2, S3) were used as substrates, and bare ITO substrate was used to fabricate a control device. The AFM images of those four substrates are shown in figure 2. The root-mean-square (RMS) of surface roughness of S1, S2, S3 was used to characterize the Ag NPs density because the single Ag NP dimensions of the three substrates are almost equal. As shown in figure 2, the RMS of S1, S2, S3 is 5.21 nm, 3.09 nm and 2.32 nm, respectively. Thus, the Ag NPs density of S1 is the highest among the substrates, then the Ag NPs density of S2, and the Ag NPs density of substrate S3 is the lowest. To investigate the influence of the thickness of the Alq_3 on the electrical characteristics of OBDs, OBDs with 100 nm, 200 nm, and 300 nm thick Alq_3 film were fabricated using substrates S1, S2, S3 and ITO, respectively. Because of different breakdown voltages for devices with different Alq_3 film thickness, the swept electrical field was kept in the range between 50 MV m^{-1} and −50 MV m^{-1} during the test for all devices. This means that the applied voltage was swept between 5 V and −5 V for the device with 100 nm thick Alq_3 film, between 10 and −10 V for the device with 200 nm thick Alq_3 film, and between 15 and −15 V for the device with 300 nm thick Alq_3 film. Current–electrical field (I–F) characteristics of OBDs were obtained by sweeping the

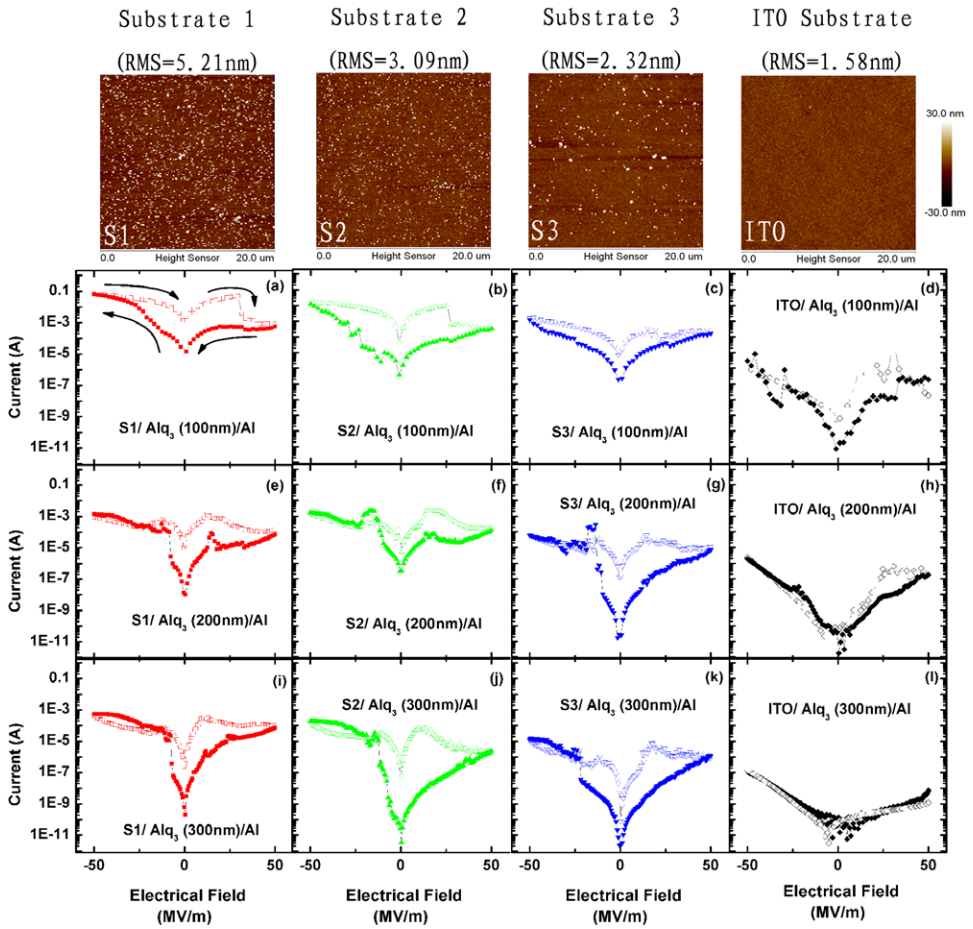

Figure 2. AFM images of the surface of ITO modified with different Ag NPs density, as well as bare ITO surface are shown in (S1), (S2), (S3) and (ITO), respectively. The root-mean-square (RMS) of surface roughness of S1, S2, S3 and ITO are 5.21 nm, 3.09 nm, 2.32 nm and 1.58 nm, respectively. (Scan size: $20 \times 20\,\mu$m) Current–electrical field (I–F) characteristics of OBDs with different Alq_3 thickness (100 nm, 200 nm, 300 nm), as well as with different substrates (S1, S2, S3, bare ITO) are shown in (a)–(l). The arrows in (a) indicate the voltage-scanning directions.

electrical field from 50 to $-50\,\mathrm{MV\,m^{-1}}$, and then from -50 to $50\,\mathrm{MV\,m^{-1}}$, as shown in figures 2(a)–(l). The influence of organic layer thickness on the switch performance of the MIM OBDs, just like structure of the control device, have been reported by many research teams [26, 38, 39]. It has been demonstrated that the switch performance became weak with the increase of organic layer thickness. Figures 2(d), (h) and (l) shows that with increase of the Alq_3 thickness, switch performance of the control device decreases. The control device with 300 nm thick Alq_3 film almost does not show a switch effect. This phenomenon coincides with the early reports very well. For OBDs using ITO modified with different density Ag NPs as substrate, as shown in figures 2(a)–(c), (e)–(g) and (j)–(k), OBDs with Alq_3 thickness varying from 100 to 300 nm all exhibit significant switching effect with high ON/OFF ratios in the range of 10^2–10^3. As the electrical field was swept from 50 to $-50\,\mathrm{MV\,m^{-1}}$, all OBDs were in OFF state at first. When the swept electrical field was close to $-50\,\mathrm{MV\,m^{-1}}$ for the device with 100 nm thick Alq_3 thickness, or to $-20\,\mathrm{MV\,m^{-1}}$ for the device with Alq_3 thickness larger than 100 nm, the OFF state switched to the ON state. When the electrical field was swept from -50 to $50\,\mathrm{MV\,m^{-1}}$, all devices were in the ON state at first. When the swept electrical field was close to $30\,\mathrm{MV\,m^{-1}}$ for the device with 100 nm thick Alq_3, or to $10\,\mathrm{MV\,m^{-1}}$ for devices with Alq_3 thickness larger than 100 nm, the ON state switched to the OFF state of the first sweep after a negative differential resistance (NDR) region. For OBDs with 100 nm thick Alq_3 film, the NDR region is formed with abrupt change of current from the ON state to the OFF state. For OBDs with Alq_3 thickness larger than 100 nm, however, the NDR region is formed with gradual decrease of current from the ON state to the OFF state. Comparing with the control devices, self-assembled Ag NPs on ITO surface (S1, S2 and S3) can enhance the conduction current of OBDs both in ON state and in OFF state significantly. With the decrease of the Ag NPs density, the conduct current decreases. Taking 100 nm thick Alq_3 devices as an example, at the electrical field of $10\,\mathrm{MV\,m^{-1}}$, the (On state, OFF state) current of devices using S1, S2, S3 and ITO as substrate were (1.6×10^{-2} A, 1.9×10^{-4} A), (3.8×10^{-3} A, 1.7×10^{-5} A), (1.6×10^{-4} A, 6.1×10^{-6} A) and (7.7×10^{-8} A, 4.4×10^{-10} A), respectively, as shown in figures 2(a)–(d). This means that Ag NPs play an important role in the conduction of the OBDs.

As shown in figure 2, it can also be noticed that the current decreases dramatically with the increase of the Alq_3 film thickness at the same electrical field and the same conduction

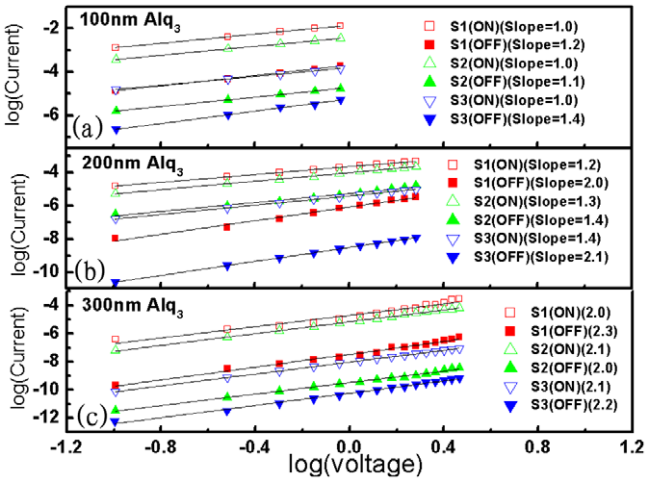

Figure 3. *I*–*V* characteristics of bistable region, which correspond to the sweep region between 0 MV m^{-1} and 10 MV m^{-1}, for OBDs with different substrates, as well as with different thickness on a logarithmic scale. (*a*)–(*c*) correspond to devices with the Alq_3 film thickness of 100 nm, 200 nm, and 300 nm, respectively. Solid lines are fitting curves for experiment data of the ON state and OFF state of these OBDs, respectively.

state for OBDs based on the same substrate. Taking electrical field with 10 MV m^{-1}, the ON state, and OBDs using S1 as substrate for example, the current of devices with 100 nm thick, 200 nm thick and 300 nm thick Alq_3 film are 1.6×10^{-2} A, 7.9×10^{-4} A and 2.1×10^{-4} A, respectively. These phenomena indicate that the current transport mechanisms in devices with different Alq_3 film are different. To elucidate the current transport mechanism of OBDs with different thickness of Alq_3 film, the current–voltage characteristics in the bistable region (the sweep region between 0 MV m^{-1} and 10 MV m^{-1}) were studied. As shown in figure 3(*a*), the current in the ON state and in the OFF state of OBDs with 100 nm thick Alq_3 all show a nearly linear-dependence on the applied voltage, which indicates an ohmic transport in both ON state and OFF state. It corresponds with the filament formation mechanism very well [10]. As shown in figure 3(*a*), the conduct current decreases with the decrease of the Ag NPs density. Thus, the Ag NPs should play an important role in the formation of conduction filament, though the physical nature of the filament is still unclear. As shown in figure 3(*b*), the current in the ON state of OBD with 200 nm thick Alq_3 shows a near linear-dependence on the applied voltage, which means this conduction state also exhibits as filament conduction. The current in the OFF state of the OBD with 200 nm thick Alq_3, however, shows a quadratic relationship with the applied voltage, which means the transport mechanism of this conduction state can be ascribed to charge storage state [33–35]. As shown in figure 3(*c*), the current in the ON state and in the OFF state of OBD with 300 nm thick Alq_3 all shows a nearly quadratic relationship with the applied voltage, which means these conduction states exhibit a charge storage mechanism, and Ag NPs should act as charge tripping sites. With the decrease of the Ag NPs density, the electric capacity decreases. Thus, the ON state current (charge process), as well as the OFF state current (discharge process), decreases with the decrease of the Ag NPs density.

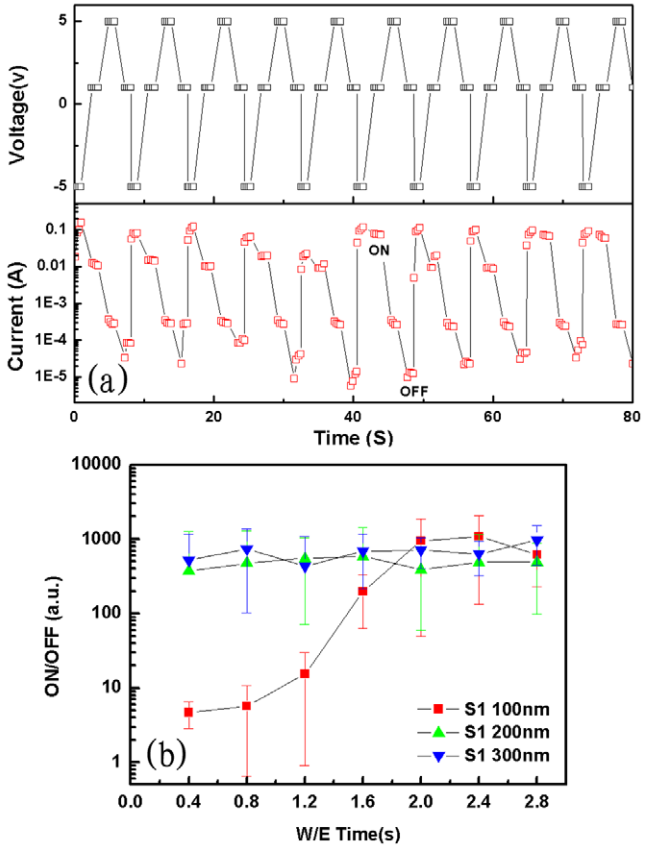

Figure 4. Applied voltage sequence, E(5 V)-R(1 V)-W(−5 V) -R(1 V), and the current response of OBD using S1 as substrate, and Alq_3 thickness of 100 nm (*a*). Average ON/OFF ratio as the function of applied time of erasure voltage and writing voltage (*b*). The ON/OFF ratio is statistical average value of 10 cycles under applied voltage sequence E(50 MV m^{-1})-R(10 MV m^{-1})-W(−50 MV m^{-1})-R(10 MV m^{-1}).

The performance of the OBDs was also investigated by applying sequential WRITE-READ-ERASE-READ voltage pulses. As shown in figure 4(*a*), taking OBDs with 100 nm thick Alq_3 and substrate S1 as representative, the current density response of the memory device followed the applied cyclic voltage sweep very well. The difference between two alternate READ currents demonstrates the ON and OFF states of the bit stored in the memory device. During the test, the applied time section of reading voltage was kept as constant of 2 s, while the applied time section of the erasure voltage and the writing voltage were equal, and varied from 0.4 to 2.8 s. Average ON/OFF ratio for OBDs (S1 substrate) with different Alq_3 thickness as the function of applied time of writing (erasure) voltage is shown in figure 4(*b*). It was shown that the value of average ON/OFF ratio increases when the applied time is prolonged for the device with 100 nm thick Alq_3 film. For the device with Alq_3 thickness larger than 100 nm, however, the average ON/OFF value did not rely on the change of applied time of the erasure voltage and the writing voltage. This phenomenon indicates that the write (erase) time that is needed to realize marked switch phenomenon for OBD with 100 nm thick Alq_3 film is much longer than that for OBD with Alq_3 thickness larger than 100 nm, which can be understood

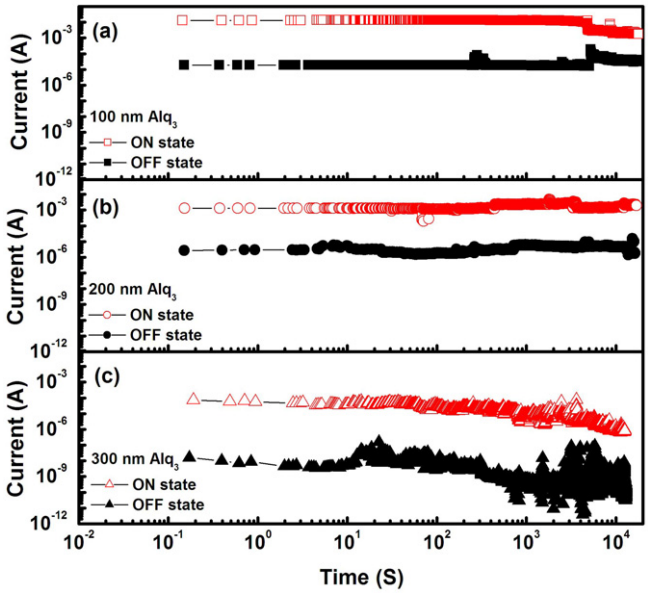

Figure 5. Data retention measurement with an electrical field of 10 MV m^{-1} of OBDs using substrate S1. The Alq_3 film thickness of 100 nm, 200 nm and 300 nm, respectively (*a*)–(*c*). The ON state and OFF state were induced by −50 MV m^{-1} and 50 MV m^{-1} pulses (width = 3 s), respectively.

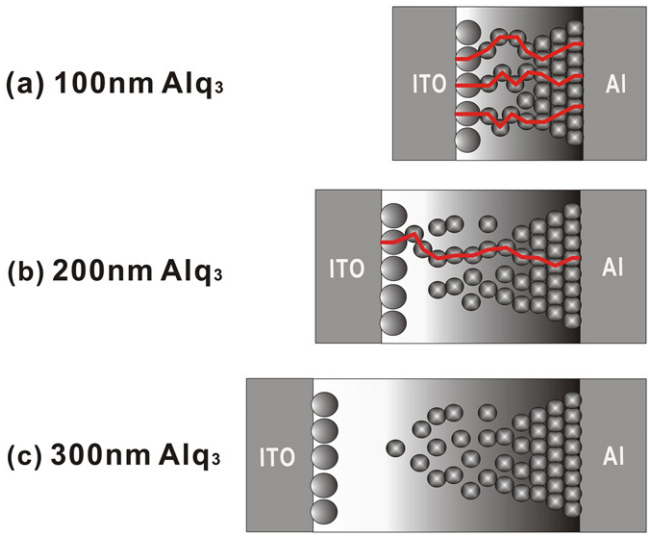

Figure 6. Schematic diagram of OBDs with different thickness of Alq_3 film. (*a*)–(*c*) The Alq_3 film thickness of 100 nm, 200 nm and 300 nm, respectively. The red solid lines show the hypothetical conducting filaments in the OBDs.

by the different switch mechanism of those OBDs. The study on the current–voltage characteristics, as shown in figure 3, have shown that OBDs with 100 nm thick Alq_3 film belong to the filament formation mechanism group, and OBDs with Alq_3 thickness larger than 100 nm belong to the charge storage mechanism group. In the filament formation mechanism, the write (erase) time corresponds with the formation (breakdown) time of filaments, which always corresponds to redox processes induced by anion or cation migration [40] and belongs to a slow process. In the charge storage mechanism, the write (erase) time corresponds with the charge (discharge) time of deep trap level, and belongs to a fast process. Thus, OBD with 100 nm thick Alq_3 film exhibited longer wirte (erase) time.

Data retention was measured under stress conditions for OBDs using S1 as substrate. The Alq_3 thickness of the OBDs were 100 nm, 200 nm, and 300 nm, respectively, as shown in figure 5. It is shown that OBDs with Alq_3 thickness less than 300 nm exhibited better data retention performance (over 10^4 s) than the OBD with 300 nm thick Alq_3. For the OBD with 300 nm thick Alq_3, strong current fluctuation occurred in the OFF state after a 2000 s test, which blurs the conductance difference between ON/OFF states. Thus, OBDs with Alq_3 thickness less than 300 nm exhibit larger potential in data-storage application.

Based on the above experimental results and discussion, we propose a phenomenological mechanism to explain the dependence of the role of Ag NPs on the thickness of the Alq_3 film. The role of Ag NPs is affected by the diffused Al atoms in the Alq_3 film. Many techniques, such as angle resolved XPS (ARXPS) [41] and medium energy ion scattering (MEIS) spectroscopy [42], have been used to study the diffuse behaviour of aluminum atoms during the evaporation of Al electrode onto the organic film. It has been reported that the concentration of diffused aluminum atoms in the organic layer decreased dramatically along the depth direction, and the diffusion length is larger than 20 nm. For OBD with 100 nm thick Alq_3 film, there are many Al atoms around Ag NPs because of the diffusion effect. Thus, the possibility of filament formed between ITO electrode and Al electrode increased, just as shown in figure 6(*a*). The switch between the ON state and the OFF state of this OBD are ascribed to the change of number of filaments. The microscopic formation process of the filaments, however, is still unknown, and further investigation is needed. For OBD with 200 nm thick Alq_3 film, there are fewer Al atoms around Ag NPs because of the limit of diffusion length of Al atoms. So, there are still a few filaments formed, but the possibility decreased, just as shown in figure 6(*b*). Thus, the ON state of this OBD exhibits filament conduction state. The OFF state of this OBD exhibits charge storage conduction state because of the decrease of filaments, as well as more trapping sites formed by isolated Ag NPs. For OBD with 300 nm thick Alq_3 film, there are almost no Al atoms around Ag NPs, just as shown in figure 6(*c*). Hence, these isolated Ag NPs act as trapping sites, and the conduction state switched with the charge or discharge of these trapping sites.

3. Conclusion

In summary, An Alq_3-based OBD using Al electrode and ITO electrode modified by Ag NPs was reported. This OBD exhibits high ON/OFF switching ratios in the range of 10^2–10^3 and long retention time over 10^4 s. The influence of the Ag NPs densities, as well as the Alq_3 film thickness on the switch performance I–V of the OBDs were studied. By analysing the I–V characteristics of OBDs with different Alq_3 film thickness, it was found that the role of the Ag NPs in the OBD depends on the thickness of the Alq_3 film. For OBD with 100 nm thick Alq_3 film, the Ag NPs acts as part of the filament

in the ON state and the OFF state. For OBD with 200 nm thick Alq_3 film, the Ag NPs act as part of the filament in the ON state, while they act as charge trapping sites in the OFF state. For OBD with 300 nm thick Alq_3 film, the Ag NPs acts as trapping sites in both ON and OFF states. A mechanism based on the diffusion effect of Al atoms in Alq_3 film was proposed to explain this dependence relationship. This work provides evidence for the connection between the filament formation mechanism and the charge storage mechanism, which is of benefit for in-depth understanding for the working mechanism of metal NPs-based OBDs.

Acknowledgments

This work was supported by Basic Research Program of China (2013CB328701-2013CB328706), National Natural Science Foundation of China (Program No 61275034), National Natural Science Young Foundation of Chian (Program No 61106123), Natural Science Basic Research Plan in Shaanxi Province of China (Program No 2012JQ8001), and the Fundamental Research Funds for the Central University (Program No xjj2012087).

References

[1] Yang Y, Ouyang J, Ma L P, Tseng R J H and Chu C W 2006 *Adv. Funct. Mater.* **16** 1001–14
[2] Scott J C and Bozano L D 2007 *Adv. Mater.* **19** 1452–63
[3] Gao X, She X J, Liu C H, Sun Q J, Liu J and Wang S D 2013 *Appl. Phys. Lett.* **102** 023302
[4] Ma L P, Liu J and Yang Y 2002 *Appl. Phys. Lett.* **80** 2997–9
[5] Bandyopadhyay A and Pal A J 2003 *Adv. Mater.* **15** 1949–52
[6] Kang S H, Crisp T, Kymissis I and Bulovic V 2004 *Appl. Phys. Lett.* **85** 4666–8
[7] Ma L P, Xu Q F and Yang Y 2004 *Appl. Phys. Lett.* **84** 4908–10
[8] Chu C W, Ouyang J, Tseng H H and Yang Y 2005 *Adv. Mater.* **17** 1440–3
[9] Verbakel F, Meskers S C J and Janssen R A J 2006 *Appl. Phys. Lett.* **89** 102103
[10] Colle M, Buchel M and de Leeuw D M 2006 *Org. Electron.* **7** 305–12
[11] Verbakel F, Meskers S C J, Janssen R A J, Gomes H L, Colle M, Buchel M and de Leeuw D M 2007 *Appl. Phys. Lett.* **91** 192103
[12] Li F, Son D I, Seo S M, Cha H M, Kim H J, Kim B J, Jung J H and Kim T W 2007 *Appl. Phys. Lett.* **91** 122111
[13] Kondo T, Lee S M, Malicki M, Domercq B, Marder S R and Kippelen B 2008 *Adv. Funct. Mater.* **18** 1112–8
[14] Lindner F, Walzer K and Leo K 2008 *Appl. Phys. Lett.* **93** 233305
[15] Liu X H, Ji Z Y, Tu D Y, Shang L W, Liu J, Liu M and Xie C Q 2009 *Org. Electron.* **10** 1191–4
[16] Chang T-Y, Cheng Y-W and Lee P-T 2010 *Appl. Phys. Lett.* **96** 043309
[17] Ouyang J Y 2013 *Org. Electron.* **14** 665–75
[18] Park Y J, Kang S J, Lotz B, Brinkmann M, Thierry A, Kim K J and Park C 2008 *Macromolecules* **41** 8648–54
[19] Lutkenhaus J L, McEnnis K, Serghei A and Russell T P 2010 *Macromolecules* **43** 3844–50
[20] Bozano L D, Kean B W, Beinhoff M, Carter K R, Rice P M and Scott J C 2005 *Adv. Funct. Mater.* **15** 1933–9
[21] Reddy V S, Karak S, Ray S K and Dhar A 2009 *Org. Electron.* **10** 138–44
[22] Tseng R J, Ouyang J, Chu C W, Huang J S and Yang Y 2006 *Appl. Phys. Lett.* **88** 123506
[23] Tseng C W, Chen Y L and Tao Y T 2012 *Org. Electron.* **13** 1436–42
[24] Lin C W, Pan T S, Chen M C, Yang Y J, Tai Y and Chen Y F 2011 *Appl. Phys. Lett.* **99** 023303
[25] Lin J and Ma D G 2008 *J. Appl. Phys.* **103** 124505
[26] Tondelier D, Lmimouni K, Vuillaume D, Fery C and Haas G 2004 *Appl. Phys. Lett.* **85** 5763–5
[27] Agrawal R, Kumar P and Ghosh S 2008 *IEEE Trans. Electron Devices* **55** 2795–9
[28] Tu C H, Lai Y S and Kwong D L 2006 *IEEE Electron Device Lett.* **27** 354–6
[29] Kang S J, Bae I, Shin Y J, Park Y J, Huh J, Park S M, Kim H C and Park C 2011 *Nano Lett.* **11** 138–44
[30] Sharma P, Reece T J, Ducharme S and Gruverman A 2011 *Nano Lett.* **11** 1970–5
[31] Hwang H J, Yang J H, Kang S C, Cho C, Kang C G, Lee Y G and Lee B H 2013 *Microelectron. Eng.* **109** 87–9
[32] Ma L P, Pyo S, Ouyang J, Xu Q F and Yang Y 2003 *Appl. Phys. Lett.* **82** 1419–21
[33] Bozano L D, Kean B W, Deline V R, Salem J R and Scott J C 2004 *Appl. Phys. Lett.* **84** 607–9
[34] Cho S H, Lee D I, Jung J H and Kim T W 2009 *Nanotechnology* **20** 345204
[35] Bo J, Zhaoxin W, Qiang H, Yuan T, Guilin M and Xun H 2010 *J. Phys. D: Appl. Phys.* **43** 035101
[36] Lukomska J, Malicka J, Gryczynski I and Lakowicz J R 2004 *J. Fluorescence* **14** 417–23
[37] Tang W, Shi H Z, Xu G, Ong B S, Popovic Z D, Deng J C, Zhao J and Rao G H 2005 *Adv. Mater.* **17** 2307
[38] Bao L, Wei Lek K, Yue S and Yang Y 2009 *Org. Electron.* **10** 1048–53
[39] Wei Lek K, Bao L, Yue S and Yang Y 2010 *Curr. Appl. Phys.* **10** e50–3
[40] Waser R and Aono M 2007 *Nature Mater.* **6** 833–40
[41] Yoshida H and Sato N 2007 *Appl. Phys. Lett.* **91** 141915
[42] Lee J H, Yi Y J and Moon D W 2008 *Appl. Phys. Lett.* **93** 153307